JAIST Repository
https://dspace.jaist.ac.jp/

Title	Effect of starting point formation on the crystallization of amorphous silicon films by flash lamp annealing
Author(s)	Sato, Daiki; Ohdaira, Keisuke
Citation	Japanese Journal of Applied Physics, 57(4S): 04FS05-1-04FS05-5
Issue Date	2018-03-01
Type	Journal Article
Text version	author
URL	http://hdl.handle.net/10119/16130
Rights	This is the author's version of the work. It is posted here by permission of The Japan Society of Applied Physics. Copyright (C) 2018 The Japan Society of Applied Physics. Daiki Sato and Keisuke Ohdaira, Japanese Journal of Applied Physics, 57(4S), 2018, 04FS05. http://dx.doi.org/10.7567/JJAP.57.04FS05
Description	

JAIST
JAPAN
ADVANCED INSTITUTE OF
SCIENCE AND TECHNOLOGY

Japan Advanced Institute of Science and Technology

Effect of starting point formation on the crystallization of amorphous silicon films by flash lamp annealing

Daiki Sato and Keisuke Ohdaira

Japan Advanced Institute of Science and Technology, Nomi, Ishikawa 923-1292, Japan

*E-mail: *ohdaira@jaist.ac.jp*

We succeed in the crystallization of hydrogenated amorphous silicon (a-Si:H) films by flash lamp annealing (FLA) at a low fluence by intentionally creating starting points for the trigger of explosive crystallization (EC). We confirm that a partly thick a-Si part can induce the crystallization of a-Si films. A periodic wavy structure is observed on the surface of poly-Si on and near the thick parts, which is a clear indication of the emergence of EC. Creating partly thick a-Si parts can thus be effective for the control of the starting point of crystallization by FLA and can realize the crystallization of a-Si with high reproducibility. We also compare the effects of creating thick parts at the center and along the edge of the substrates, and a thick part along the edge of the substrates leads to the initiation of crystallization at a lower fluence.

1. Introduction

In recent years, solar power generation has attracted much attention as a solution to environmental problems such as global warming. Crystalline silicon (c-Si) solar cells using Si wafers have been generally used because of their high stability for light soaking and high conversion efficiency. However, they need a large amount of Si material, leading to a high production cost. Thin-film poly-Si solar cells have thus been expected as low-cost, next-generation solar cells, since they can lower the usage of Si material and low-cost substrates such as glass can be utilized.[1–9] There are many methods used to form poly crystalline Si (poly-Si) on glass substrates, such as the crystallization of precursor amorphous Si (a-Si) films and the direct deposition of microcrystalline Si (μc-Si) films. Among these methods, we have focused on the crystallization of a-Si by flash lamp annealing (FLA),[10–28] millisecond-order annealing using pulse light from xenon lamps.[29–31] FLA can crystallize μm-order-thick a-Si films without serious thermal damage to glass substrates with poor thermal tolerance because of the thermal diffusion length being several tens of μm both for a-Si and glass.[10] If we form poly-Si films by the FLA of hydrogenated a-Si films prepared by catalytic chemical vapor deposition (Cat-CVD), sufficiently long minority carrier lifetimes can be realized after successive postannealing.[21,24] We have also demonstrated the operation of a p-i-n solar cell with a poly-Si film formed by FLA as an absorber.[26] The crystallization of μm-order-thick a-Si films by FLA is known to be continuous in the lateral direction owing to heat generation and diffusion, originating from enthalpy difference between a-Si and c-Si. This particular crystallization is referred to as explosive crystallization (EC).[32] The EC of a-Si films induced by FLA tends to start from the edges of the films, probably because the edges receive additional irradiation from angled flash-lamp pulse light[12] and are thus heated more than the other parts. However, at present, the reproducibility of the crystallization of a-Si films by FLA is insufficient because the starting point of crystallization is not controlled.

In this study, we have attempted to control the starting point of crystallization. In our previous work, we have clarified that thick a-Si films tend to be crystallized at a low fluence of a flash lamp pulse[10]. On the basis of this result, if we perform FLA on partly thick a-Si films, the thick part is expected to be crystallized first, which leads to the release

of heat corresponding to enthalpy difference between the a-Si and c-Si phases, and EC may be triggered there. We have thus investigated the effect of intentionally creating thick a-Si parts on the crystallization of a-Si films by FLA, by comparing a-Si films without thick a-Si parts. We have also compared the samples with thick a-Si parts along the edges, partly reported in our previous work[28], with those with thick a-Si parts at the center of the substrates to obtain a more significant effect for the initiation of EC.

2. Experimental methods

We used alkali-free (Corning Eagle XG) flat glass substrates with dimensions of 19.8 × 19.8 × 0.4 mm^3. We first performed the ultrasonic cleaning of the glass substrates in Semicoclean, ethanol, and deionized water for ~10 min, respectively. ~200-nm-thick Cr films were then deposited on the glass substrates by sputtering. The Cr films were used only to prevent the peeling of Si films during FLA[26] and there is no critical effect on the crystallization of a-Si.[13] We then deposited a-Si films with a thickness of 2 μm at the center or along the edges of the substrates by sputtering using a metal mask or a glass plate. The sputtering of a-Si films was performed at a pressure of 1.1 Pa and at an Ar flow rate of 40 sccm. The reason for the utilization of sputtered a-Si films in the thick parts is the low fluence of the flash lamp pulse required for crystallization than in the case of Cat-CVD a-Si.[27] After partly depositing a-Si films, hydrogenated a-Si films were deposited on the entire surfaces of the substrates by Cat-CVD at a catalyzer temperature of 1800±50 °C, a substrate holder temperature of 200 °C, and at SiH_4 and H_2 flow rates of 50 and 10 sccm, respectively. The schematic images of precursor a-Si structures are shown in Fig. 1. FLA was performed by irradiating a 7-ms-duration flash lamp pulse with various fluences from a Xe lamp to the samples preheated at 500 °C in Ar atmosphere. The pulse light emitted from the Xe lamp has a broad spectrum mainly in the visible region, as reported previously.[25] Only one flash lamp pulse was irradiated for each sample. The surfaces of Si films after FLA were observed by optical microscopy. We also evaluated the grain size and crystalline fraction of Si films by Raman spectroscopy using the 632.8 nm line of a He-Ne laser. We confirmed that the intensity of the laser light is insufficient for inducing the crystallization of a-Si films and that the irradiation of the laser light does not affect the crystalline fraction

of Si films. The full width at half maximum (FWHM) of a c-Si Raman peak obtained from a reference c-Si wafer was ~3.5 cm^{-1}. We calculated the crystalline fraction (X_c) of poly-Si films as

$$X_c = \frac{I_g + I_c}{I_g + I_c + I_a},$$

where I_g, I_c, and I_a represent the peak integrals of Raman signals from the grain boundary (~500 cm^{-1}), c-Si (~520 cm^{-1}), and a-Si (~480 cm^{-1}), respectively. We also examined the entire crystallization of a thick a-Si part after FLA along the depth direction by repeating Raman measurement and etching in a mixed solution of hydrofluoric acid (HF), nitric acid (HNO_3), and deionized water ($HF:HNO_3:H_2O$=1:50:50).

3. Results and discussion

Figures 2(a) and 2(b) show the surface images of Si films with thick parts along the substrate edges after FLA at fluences of 9.27 and 11.7 J/cm^2, respectively. The surface image of a Si film without a thick part after FLA at a fluence of 11.7 J/cm^2 is also shown for comparison in Fig. 2(c). Figure 2(d) shows that of a Si film with a thick part at the center of the substrate after FLA at a fluence of 12.4 J/cm^2, in which the region indicated by a circle is the thick part. In Figs. 2(b) and 2(c), regions (2), (3), and (4) indicate a thin crystallized part starting from a thick part, a thick part along the edge of the substrate, and a thin part in the sample without a thick part, respectively. In the case of a fluence of 9.27 J/cm^2, only the thick part [region (1)] is crystallized, which was confirmed both by the color change of the Si surface and by Raman spectroscopy. This indicates that a thick part is crystallized at a lower fluence than a thin part, which is consistent with our previous result.[10)] It can be seen that lateral crystallization starts from the thick part in Fig. 2(b) when the fluence of a flash lamp pulse is increased to 11.7 J/cm^2. In Fig. 2(d), regions (5), (6), and (7) show a thin crystallized part from a thick part, the thick part at the center of the substrate, and a thin crystallized part from the other part, respectively. As in the case of the samples with a thick part along the substrate edge, we can confirm the crystallization of thin a-Si parts starting from the thick part. In this precursor structure, crystallization from the thick part starts to occur at a fluence of 12.4 J/cm^2. We have confirmed a similar crystallization of a-Si starting

from thick parts in more than ten samples in both precursor structures, indicating a high reproducibility.

We have also performed the FLA of a-Si films for three different precursors at various fluences, whose surface images are not shown here. When the fluence of the flash lamp pulse is increased, crystallization starts not only from the thick a-Si parts but from other substrate edges for all the samples, as reported previously.[12] The complete crystallization of entire a-Si films is confirmed at a sufficiently high flash pulse fluence. Note that precursor a-Si films without thick a-Si parts are partly crystallized only when the fluence of the flash lamp pulse is 13.2 J/cm^2 or more, which is much higher than those for the samples with thick a-Si films.

Figure 3 shows the Raman spectra of Si films measured in regions (2), (3), and (4). The sample with a thick part along the substrate edge shows peaks at ~519 cm^{-1}, originating from the c-Si phase, while only a peak at ~480 cm^{-1} from the a-Si phase is seen in the sample without a thick part. Note that the thin part near the thick part is also crystallized, as indicated in the Raman spectrum of region (2). Figure 4 shows the Raman spectra of Si films measured in regions (5), (6), and (7). These spectra show peaks at ~519 cm^{-1}, and both the thick part and the thin part near the thick part are thus crystallized. We can therefore conclude that the creation of a thick part in a precursor a-Si film induces the crystallization of thin a-Si films. The Raman spectra of the crystallized parts in this work have c-Si peaks at ~519 cm^{-1}, showing a wavenumber shift that is ~1 cm^{-1} lower than that of a c-Si wafer of ~520.5 cm^{-1}. This indicates that the poly-Si films have a tensile stress.[33] This tensile stress is not due to the original stress of precursor a-Si films since the sputtered films have a strongly compressive stress[27] and the Cat-CVD films deposited at a substrate temperature of 200 °C have a weakly compressive stress.[16, 17] Unlike in the case of a-Si films fully covering substrate surfaces, partly formed a-Si can relax its stress. Furthermore, Si films become more compact through crystallization, which can lead to the emergence of tensile stress. These may be the reasons for the existence of a tensile stress in the poly-Si films formed. The Raman spectra measured in regions (2), (3), and (5)–(7) show c-Si peaks with an FWHM of ~7 cm^{-1}, which is larger than that of a reference c-Si wafer. This indicates that poly-Si films in these regions consist of fine grains with a size of ~10 nm.[32]

The crystalline fractions obtained from the Raman spectra of these regions are >80%, indicating the formation of poly-Si films with high crystallinity.

We also investigated the crystallization of the thick a-Si part along the depth direction. Figures 5(a) and 5(b) show the Raman spectra of thick Si parts measured at various thicknesses. The values of the figures indicate the distances from the original film surfaces, and the spectra with values in 0–2 μm are from Cat-CVD parts and those with values >2 μm are from sputtered parts. All the Raman spectra are composed mainly of c-Si peaks at ~520 cm^{-1}, indicating the complete crystallization of thick a-Si parts by one flash pulse irradiation. This fact means that the bottom sputtered a-Si can generate and supply heat to initiate the crystallization of surrounding thin Cat-CVD a-Si films.

Figure 6 shows the optical microscopic images of the surfaces of Si films after FLA. We have thus far clarified that periodic wavy structures with a spacing of ~1 μm grow along the lateral crystallization direction on the surfaces of poly-Si films if the poly-Si films are formed through a particular mode of EC in which solid-phase nucleation and liquid-phase epitaxy alternatively occur.[12] Similar wavy structures are also seen on the surfaces of poly-Si films formed by the FLA of a-Si films with thick parts. The wavy structures are seen on the surfaces of both the thick part and the thin part crystallized from the thick part. This means that the lateral crystallization that started from the thick part is based on the EC described above, and that the thick part can act as the starting point for EC.

We next compare the FWHM of Raman c-Si peaks, crystalline fraction, and fluence required for the formation of poly-Si films with thick parts at the center and edge of the films, which are summarized in Table I. We can see no significant differences in FWHM (~7 cm^{-1}) and crystallinity (>80%) for poly-Si films formed from precursor a-Si films with thick parts at the center and along the side of the substrates. We can thus consider that the position of thick parts does not affect the quality of poly-Si films. On the other hand, the fluence of the flash lamp pulse required for crystallization from the thick parts can be lowered from 12.4 to 11.7 J/cm^2 by creating the thick part along the edge of the substrates compared with the case of the samples with the thick part at the center. Creating the thick part along the edge of the substrates is therefore more effective for triggering EC. This may be due to the angled flash lamp light irradiation of the edges of precursor a-Si films.[12] Because the angled flash lamp light irradiation of the edge of the substrates does not reach

the a-Si parts far from the edges, the temperature of the edge parts of a-Si becomes higher than that of the interior part under the same FLA fluence. This may be the reason for the initiation of EC even in the case without the thick a-Si part along the edges. By thickening the edge parts of a-Si films, the temperature of the edge parts increases more easily, resulting in the crystallization there at a low fluence. The thick part of a-Si along the edges of the substrates can act as the starting point of EC more effectively.

Finally, we discuss the application of creating thick a-Si parts to the formation of large-area poly-Si films. As mentioned above, we have clarified that creating thick a-Si parts can control the initiation of EC. Although creating thick a-Si parts along the substrate edges is more effective for initiating EC, the length of EC during FLA from the substrate edges is limited to a few cm, on the basis of an EC velocity of ~4 m/s[22, 23] and a pulse duration <10 ms. This means that EC regions from the edges cannot completely cover the entire area of large-area Si films with a size of several tens of cm or more. Thus, creating thick a-Si parts in the interior of a-Si films will also be necessary for the formation of large-area poly-Si films. Thick poly-Si parts will be formed in the interior parts after FLA in this structure, which may be harmful for the performance of solar cells. One possible way to remove the thick poly-Si parts is laser scribing. If the thick a-Si parts are prepared along the laser scribing lines that are originally required for the fabrication of superstrate-type solar cells, no additional process is required for the removal of thick poly-Si films. Note that the utilization of much thicker poly-Si films is favorable for the application of the poly-Si films formed by FLA to actual solar cells. We have already confirmed the formation of 10-μm-thick poly-Si films by FLA,[23] and there is no technical difficulty in the formation of thicker poly-Si films.

4. Conclusions

We have investigated the effect of creating partially thick a-Si parts on the initiation of EC by FLA. We have confirmed that crystallization can start from the thick parts, and the crystallization is based on EC. Creating the thick parts on the substrates can trigger the EC of surrounding thin a-Si films. In addition, creating the thick a-Si part along the substrate

edge realizes crystallization at a lower fluence. The creation of the thick a-Si parts will contribute to the crystallization of a-Si films by FLA with high reproducibility at low fluences even in large-scale substrates.

Acknowledgment

This work was supported by JSPS KAKENHI Grant Number 15H04154.

References

1) M. A. Green, Sol. Energy **74**, 181 (2003).
2) W. Fuhs, S. Gall, B. Rau, M. Schmidt, and J. Schneider, Sol. Energy **77**, 961 (2004).
3) M. Spitzer, J. Schewchun, E. S. Vera, and J. J. Lofersky, Proc. 14th IEEE Photovoltaic Specialists Conf., 1980, p. 375.
4) A. A. D. T. Adikaari, N. K. Mudugamuwa, and S. R. P. Silva, Sol. Energy Mater. Sol. Cells **92**, 634 (2008).
5) J. K. Saha, K. Haruta, M. Yeo, T. Koabayshi, and H. Shirai, Sol. Energy Mater. Sol. Cells **93**, 1154 (2009).
6) T. Matsuyama, M. Tanaka, S. Tsuda, S. Nakano, and Y. Kuwano, Jpn. J. Appl. Phys. **32**, 3720 (1993).
7) M. J. Keevers, T. L. Young, U. Schubert, and M. A. Green, Proc. 22nd European Photovoltaic Solar Energy Conf., 2007, p. 1783.
8) I. Gordon, L. Carnel, D. Van Gestel, G. Beaucarne, J. Poortmans, L. Pinckney, and A. Mayolet, Proc. 22nd European Photovoltaic Solar Energy Conf., 2007, p. 1993.
9) S. Arimoto, H. Morikawa, M. Deguchi, Y. Kawama, Y. Matsuno, T. Ishihara, H. Kumabe, and T. Murotani, Proc. 24th IEEE Photovoltaic Specialists Conf., 1994, p. 1311.
10) K. Ohdaira, S. Nishizaki, Y. Endo, T. Fujiwara, N. Usami, K. Nakajima, and H. Matsumura, Jpn. J. Appl. Phys. **46**, 7198 (2007).
11) K. Ohdaira, T. Fujiwara, Y. Endo, S. Nishizaki, and H. Matsumura, Jpn. J. Appl. Phys. **47**, 8239 (2008).
12) K. Ohdaira, T. Fujiwara, Y. Endo, S. Nishizaki, and H. Matsumura, J. Appl. Phys. **106**, 044907 (2009).

13) K. Ohdaira, Y. Endo, T. Fujiwara, S. Nishizaki, and H. Matsumura, Jpn. J. Appl. Phys. **46**, 7603 (2007).
14) K. Ohdaira, T. Nishikawa, K. Shiba, H. Takemoto, and H. Matsumura, Thin Solid Films **21**, 518 (2007).
15) K. Ohdaira and H. Matsumura, Thin Solid Films **524**, 161 (2012).
16) K. Ohdaira and T. Watanabe, Thin Solid Films **595**, 235 (2015).
17) K. Ohdaira, Thin Solid Films **575**, 21 (2015).
18) K. Ohdaira, T. Fujiwara, Y. Endo, K. Nishioka, and H. Matsumura, J. Cryst. Growth **311**, 769 (2009).
19) K. Ohdaira, T. Nishikawa, and H. Matsumura, J. Cryst. Growth **312**, 2834 (2010).
20) K. Ohdaira, T. Nishikawa, K. Shiba, H. Takemoto, and H Matsumura, Phys. Status Solidi C **7**, 604 (2010).
21) K. Ohdaira, H. Takemoto, T. Nishikawa, and H. Matsumura, Curr. Appl. Phys. **10**, S402 (2010).
22) K. Ohdaira, N. Tomura, S. Ishii, and H. Matsumura, Electrochem. Solid-State Lett. **14**, H372 (2011).
23) K. Ohdaira, Can. J. Phys. **92**, 718 (2014).
24) K. Ohdaira, H. Takemoto, K. Shiba, and H. Matsumura, Appl. Phys. Express **2**, 061201 (2009).
25) K. Ohdaira, Jpn. J. Appl. Phys. **52** 04CR11 (2013).
26) K. Ohdaira, T. Fujiwara, Y. Endo, K. Shiba, H. Takemoto, and H. Matsumura, Jpn. J. Appl. Phys. **49**, 04DP04 (2010).
27) K. Ohdaira, S. Ishii, N. Tomura, and H. Matsumura, J. Nanosci. Nanotechnol. **12**, 591 (2012).
28) D. Sato and K. Ohdaira, Ext. Abst. 2017 Int. Conf. Solid State Devices and Materials (SSDM2017), 2017, C-1-03.
29) B. Pétz, L. Dobos, D. Panknin, W. Skorupa, C. Lioutas, and N. Vouroutzis, Appl. Surf. Sci. **242**, 185 (2005).
30) F. Terai, S. Matsunaka, A. Tauchi, C. Ichikawa, T. Nagatomo, and T. Homma, J. Electrochem. Soc. **153**, H147 (2006).
31) H. Habuka, A. Hara, T. Karasawa, and M. Yoshioka, Jpn. J. Appl. Phys. **46**, 937 (2007).

32) H.-D. Geiler, E. Glaser, G. Gotz, and M. Wagner, J. Appl. Phys. **59**, 3091 (1986).
33) A. A. Sirenko, J. R. Fox, I. A. Akimov, X. X. Xi, S. Ruvimov, and Z. Liliental-Weber, Solid State Commun. **113**, 553 (2000).
34) C. Smit, R. A. C. M. M. van Swaaij, H. Donker, A. M. H. N. Petit, W. M. M. Kessels, and M. C. M. van de Sanden, J. Appl. Phys. **94**, 3582 (2003).

Table I. FWHM of Raman c-Si peaks, crystalline fraction of poly-Si formed by the crystallization of a-Si films with thick parts at their center and edge. The flash lamp pulse fluences required for the crystallization of these a-Si films are also shown.

	Center		Edge	
	Thick part	Crystallized region starting from thick part	Thick part	Crystallized region starting from thick part
FWHM (cm^{-1})	6.68±0.94	6.73±0.57	6.38±0.86	5.91±0.40
X_c (%)	87.3	86.8	85.8	92.6
Fluence required for crystallization (J/cm^2)	12.4		11.7	

Figure Captions

Fig. 1. (Color online) Schematics of precursor a-Si structures with thick parts along the edge [(a) and (c)] and center [(b) and (d)] of the substrates. (a) and (b) are the schematics without Cat-CVD a-Si films, and (c) and (d) are those with Cat-CVD a-Si films.

Fig. 2. (Color online) Surface images of the samples with a thick part at the edge of the substrate after FLA at fluences of (a) 9.27 and (b) 11.7 J/cm^2, (c) without thick part after FLA at a fluence of 12.4 J/cm^2, and (d) at the edge of the substrate after FLA at a fluence of 12.4 J/cm^2. Regions (1), (3), and (6) are thick parts, regions (2) and (5) are crystallized parts starting from the thick parts, region (4) is a part of the sample without a thick part, and region (7) is a crystallized part not starting from the thick part. A white circle in (d) indicates the thick part.

Fig. 3. Raman spectra of Si films with and without a thick part at the edge of the substrate: (2) crystallized part starting from the thick part, (3) thick part, and (4) a Si film without thick part.

Fig. 4. Raman spectra of Si films with a thick part at the center of the substrate: (5) crystallized part from the thick part, (6) thick part, and (7) crystallized part from other part.

Fig. 5. Raman spectra of the thick part of a Si film formed at (a) the edge and (b) center of the substrate. The values in the figures indicate the distances from the original film surfaces.

Fig. 6. (Color online) Optical microscopic images of the surfaces of poly-Si films formed from a-Si with the thick parts at the edge [(a) and (b)] and center [(c) and (d)] of the substrate. (b) and (d) are the images in regions near the thick parts and (a) and (c) are those at the thick parts.

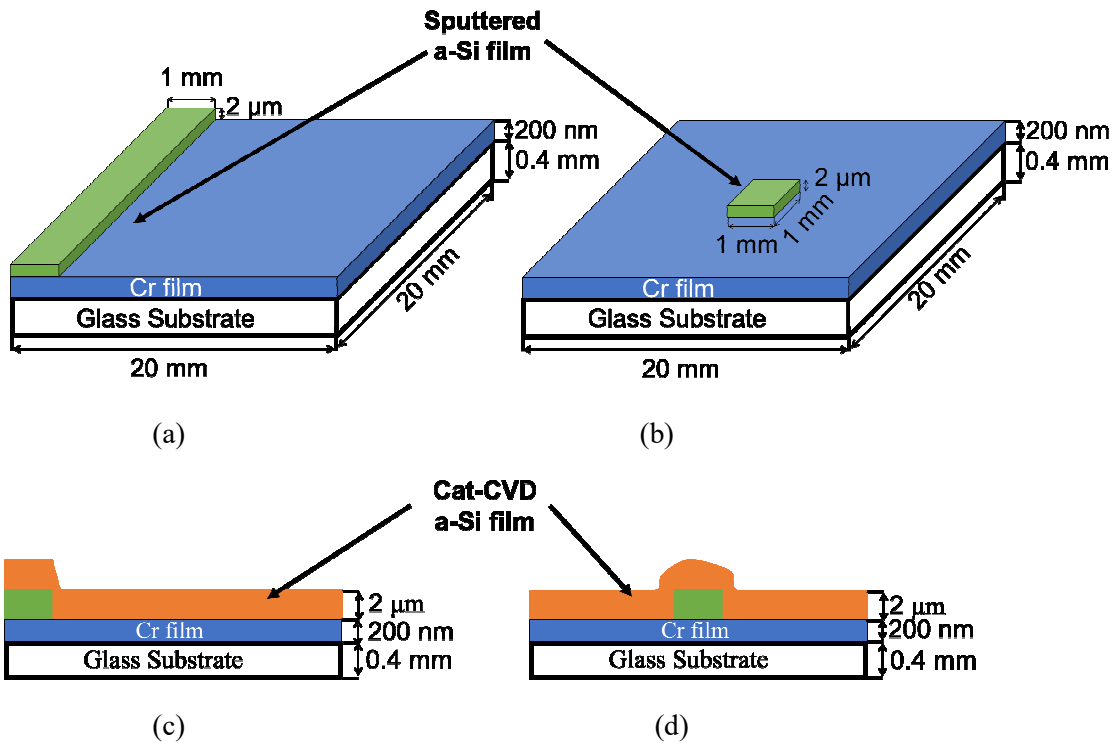

Fig.1. (Color Online) D. Sato *et al*.

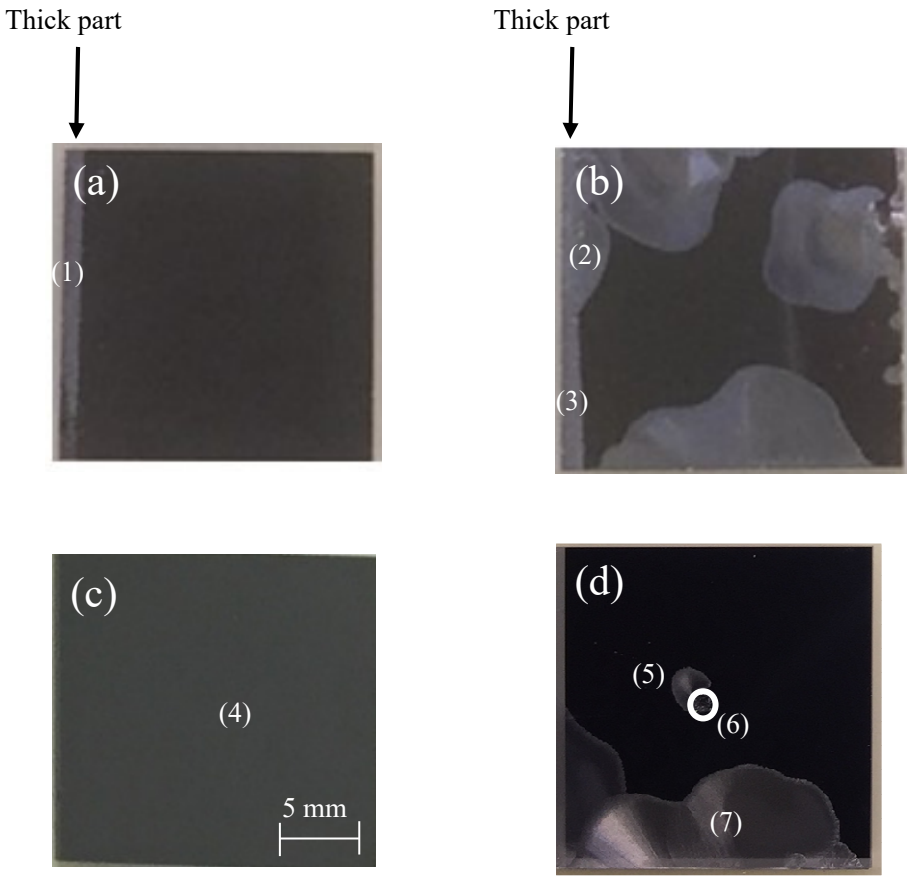

Fig. 2. (Color Online) D. Sato *et al*.

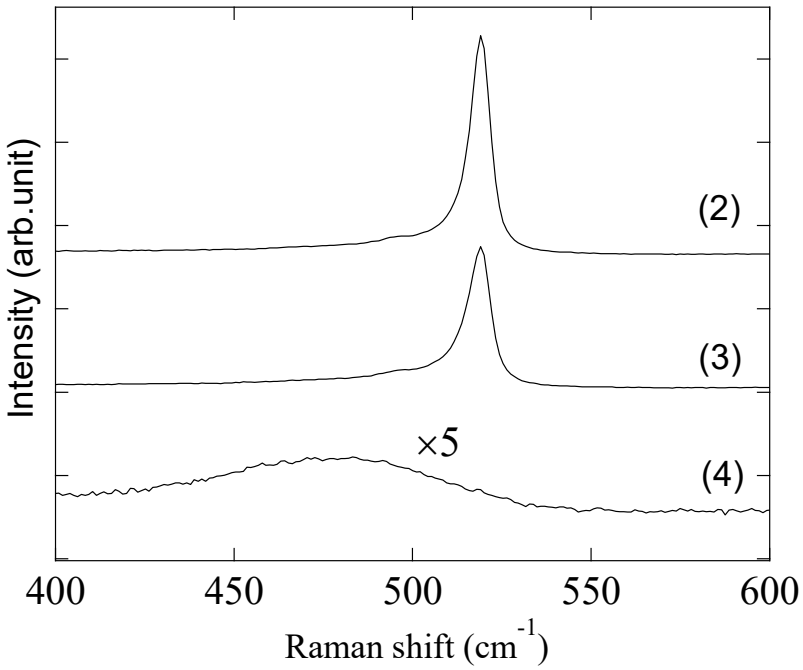

Fig. 3. (Color Online) D. Sato *et al*.

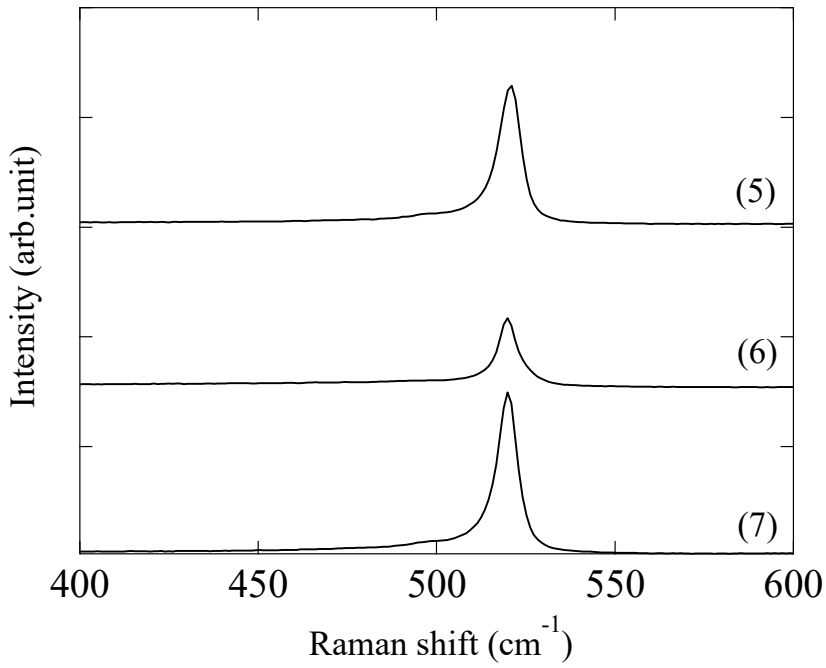

Fig. 4. (Color Online) D. Sato *et al*.

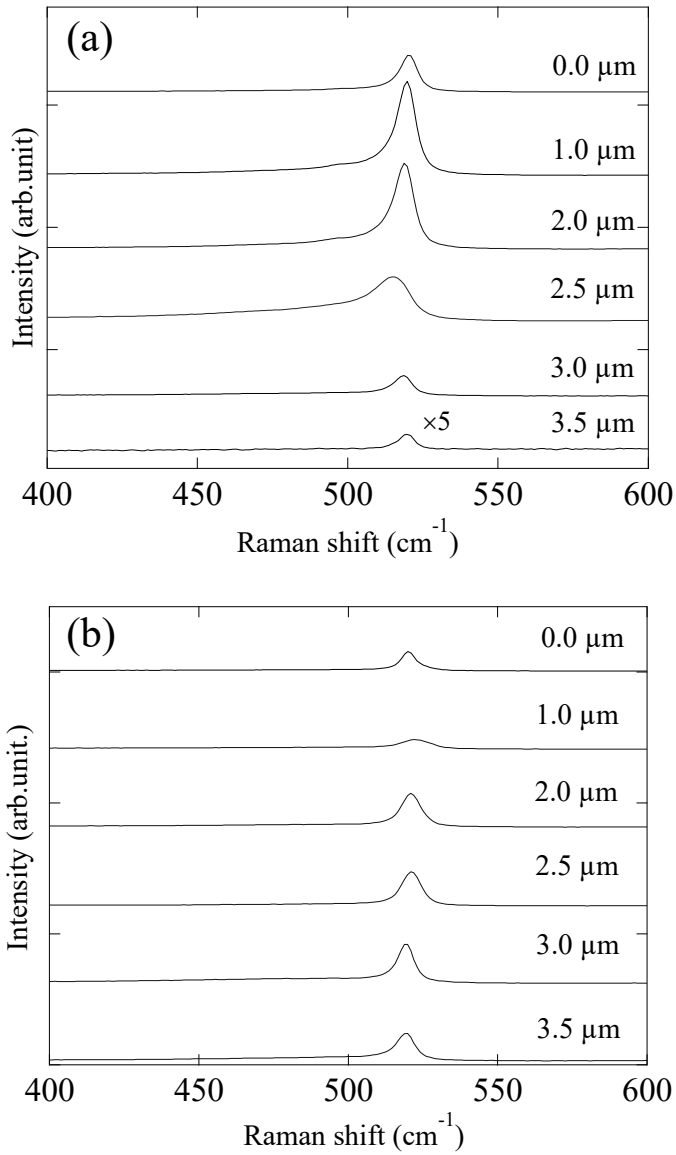

Fig. 5. D. Sato *et al*.

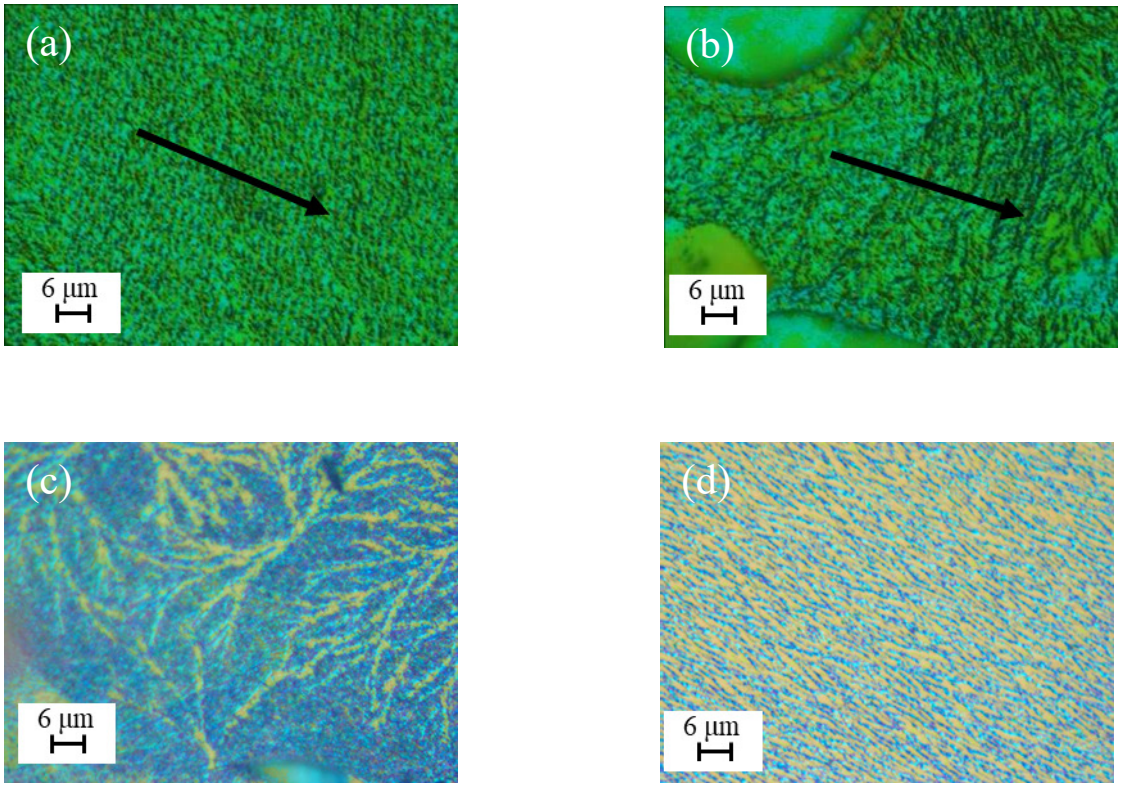

Fig. 6. (Color Online) D. Sato *et al*.